

Electronic properties of K-doped C₆₀(111): Photoemission and electron correlation

P. J. Benning, F. Stepniak, D. M. Poirier, J. L. Martins, and J. H. Weaver

Department of Materials Science and Chemical Engineering, University of Minnesota, Minneapolis, Minnesota 55455

L. P. F. Chibante and R. E. Smalley

Rice Quantum Institute and Departments of Chemistry and Physics, Rice University, Houston, Texas 77251

(Received 3 December 1992)

High-resolution photoemission provides the signatures of K₃C₆₀(111), K₄C₆₀, K₆C₆₀, and the dilute solid solution of K in C₆₀(111), showing the effects of electron-electron correlation in all of the K-C₆₀ phases. K₃C₆₀(111) is a metal with a distinct Fermi-level cutoff but with spectral broadening near E_F not predicted by band calculations. K₄C₆₀ is an insulator, although band calculations predict metallic character. Photoemission and low-energy-electron-diffraction results demonstrate kinetically limited growth for K-C₆₀ films produced by vapor deposition.

Spectroscopic results have offered conflicting views of the electronic states of K_xC₆₀ near the Fermi level (E_F), especially for $x \approx 3$.^{1,3,4} In particular, several photoemission studies^{1,3,5} have suggested metallic character for K₃C₆₀, and the results have been interpreted in a one-electron picture.³ Other studies^{2,5} have found very little emission at E_F , leading one group to conclude that K₃C₆₀ exhibits a pseudogap⁵ at E_F , and there has even been speculation that K₃C₆₀ should be a Mott-Hubbard insulator.⁶ Motivated by the lack of a clear consensus, we have undertaken photoemission studies of highly crystalline K_xC₆₀ films at low temperature, providing the best combination of sample quality and experimental resolution employed thus far. C₆₀(111) films were grown epitaxially on GaAs(110), as demonstrated by low-energy electron diffraction (LEED) and scanning tunneling microscopy (STM). Photoemission studies were conducted with three different photon energies, providing a range of probe depths and assuring an accurate determination of the doping level. These conditions have allowed us to isolate the K₃C₆₀ and K₄C₆₀ valence-band spectra. We find that oriented single crystals of K₃C₆₀ are produced in coexistence with a solid solution phase at low doping. K₃C₆₀ is clearly metallic, but the lowest unoccupied molecular orbital (LUMO)-derived structure is much broader than predicted by one-electron band theory.⁷ K₄C₆₀, previously unreported for thin-film experiments, nucleates before x reaches 3. This indicates that fullerene growth by vapor-phase deposition follows a nonequilibrium path. K₄C₆₀ is an insulator with a lower Hubbard band centered 0.5 eV below E_F . Both phases demonstrate the importance of electron correlation, as for C₆₀ and K₆C₆₀.^{6,8,9} Although these films are laterally heterogeneous, there is no evidence of a unique surface electronic spectrum.

Films of C₆₀ ~ 200 Å thick were prepared by condensation onto cleaved GaAs(110) at 180 °C to optimize crystal growth. Thicknesses were calibrated by measuring the attenuation rate of substrate emission features using x-ray photoemission (XPS). A quartz-crystal-thickness monitor indicated that the sticking coefficient was ~0.2 at

180 °C; it was too low at 200 °C for film growth. Potassium was sublimed from SAES getter sources at pressures below 2×10^{-10} Torr. The C₆₀ films were held at 180 °C during K deposition. The K_xC₆₀ stoichiometries were determined from K 2*p* and C 1*s* core-level and LUMO intensities, assuming a saturated composition of K₆C₆₀. The estimated uncertainty in x was ±0.2. Photoemission ($h\nu = 1486.6, 21.2, \text{ and } 16.8 \text{ eV}$) and LEED measurements were conducted concurrently. The ultraviolet photoemission (UPS) resolution was 100 meV, including thermal broadening, based on the 10–90 % step height at E_F . The spectra discussed here were collected at 40 K, although spectra obtained at higher temperatures differed only in the extent of thermal broadening.

LEED studies using four-grid Varian optics showed a hexagonal pattern for C₆₀ at 40 K, consistent with a simple cubic C₆₀(111) surface having a basis of four molecules.¹⁰ The diffraction pattern showed orientationally ordered grains with C₆₀[110] rotated ~3° with respect to GaAs[111]. The pattern was unchanged as the electron spot was moved across the surface. STM studies of films grown under identical conditions showed grain sizes exceeding 3500 Å, the largest scan window used to investigate fullerene growth. A LEED pattern that reflected the fcc phase (a hexagonal pattern with spot separations twice that of the sc phase) was observed upon warming, consistent with orientational disorder of C₆₀ in the solid state.¹⁰ Doping with K to nucleate K₃C₆₀ produced the fcc hexagonal pattern across the sample surface for $40 < T < 300 \text{ K}$. The intensity of the K₃C₆₀ pattern increased as x was increased from ~0.9 to ~2.5. The lower limit reflected our ability to see the pattern easily. The LEED intensity decreased at higher x ; it was visible at $x = 3.9$ but was not for $x > 4$. This behavior can be explained in terms of the phases identified in x-ray-diffraction studies.¹¹ Doping of C₆₀(111) produces ordered K₃C₆₀(111) grains, giving the hexagonal pattern, but the lattice expansion necessary for transformation to bct K₄C₆₀ introduces surface roughness, compromising the diffraction conditions. This surface roughness has also been observed in STM studies.¹²

The UPS spectra of Fig. 1 for K_xC_{60} are referenced in energy to the grounded spectrometer Fermi level. They are normalized to the integrated emission intensity from the band derived from the highest occupied molecular orbital (HOMO) of C_{60} , i.e., the peak ~ 2.5 eV below E_F . The occupation of a LUMO-derived band with electrons donated from K atoms in interstitial sites is indicated by the increasing emission within 1.5 eV of E_F .^{1-5,8} The spectra of Fig. 1 exhibit better-resolved structure compared to Refs. 1-5 because of improved crystallinity and/or reduced phonon broadening, and make possible analysis that reveals the signatures of the K_3C_{60} and K_4C_{60} phases. We see no evidence of the pseudogap reported in Ref. 5. Instead, there is a distinct Fermi cutoff, as in Refs. 3 and 4, and our results show additional structure in the LUMO feature 0.3 and 0.7 eV below E_F , suggesting a correlated system rather than a simple metal.

The $x=0.1$ spectrum is dominated by emission from the solid solution phase, $\alpha-C_{60}(111)$. Emission at E_F and a shoulder at ~ 1.6 eV are due to small amounts of K_3C_{60} . The HOMO and HOMO-1 bands are broader than for C_{60} because of K disorder, reflecting a range of spectral functions. The Fermi-level emission and the 1.6-eV shoulder increase with doping until $x \sim 2.2$. Significantly, the spectral shape in the LUMO region within ~ 1.5 eV of E_F is essentially unchanged from $x=0.1$ to 2.2. These spectral features are derived from

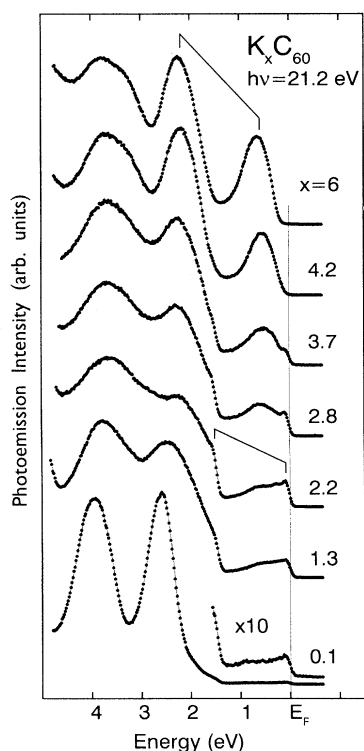


FIG. 1. UPS spectra showing a sharp Fermi level cutoff when the K_3C_{60} phase is present and no emission at E_F for the K_4C_{60} phase. The $x=6$ spectrum was shifted 0.2 eV toward E_F to facilitate comparison to the lower spectra.

K_3C_{60} . The change in intensity is that expected for a two-phase sample with varying global composition but fixed phases. The HOMO and HOMO-1 features are broad because of overlapping contribution from the two phases, offset by ~ 0.6 eV. The $x=2.8$ spectrum shows a new feature centered 0.5 eV below E_F that announces the nucleation of K_4C_{60} . The K_4C_{60} signatures dominate by $x=3.7$ and the K_3C_{60} contributions have vanished by $x=4.2$. Additional K incorporation produces slight changes in the valence-band emission features as the bcc K_6C_{60} is formed and the LUMO intensity increases to its saturated value.⁸

Previous photoemission studies have not identified the K_4C_{60} phase, and it has even been speculated that this phase does not form in thin films. Here we associate the spectra for $x=4.2$ with the K_4C_{60} phase based on the line shapes and intensities of the LUMO and core-level features. If the $x=4$ phase did not exist, then the disappearance of K_3C_{60} (characterized by loss of emission at E_F) would require that a predominantly K_6C_{60} film be composed of $\sim 35\%$ $\alpha-C_{60}$ to obtain an overall stoichiometry of $K_{4.2}C_{60}$. This situation can be ruled out since no evidence of the $\alpha-C_{60}$ HOMO-derived features is seen in the sharp features of the $x=4.2$ spectrum. (They would appear shifted 0.4 eV to higher binding energy relative to those in the $x=4.2$ spectrum, producing extreme broadening.) Moreover, the K $2p$ features show the complete loss of emission characteristic of the K_3C_{60} phase when the film stoichiometry is K_4C_{60} , and LEED studies show the disappearance of the K_3C_{60} pattern at $x=4$. Resistivity measurements¹³ as a function of K concentration reveal a sharp increase in $\rho(x)$ between $x=3$ and 4 and a more gradual increase between $x=4$ and 6. Hence, we conclude that the $x=4.2$ spectrum is representative of a K_4C_{60} phase, presumably with the bct structure identified by x-ray-diffraction studies.

The appearance of K_4C_{60} before $x=3$ and its coexistence with the α and K_3C_{60} phases demonstrates that films grown by vapor deposition do not achieve true thermodynamic equilibrium.¹⁴ In particular, only two phases can coexist for a two-component system under conditions of thermodynamic equilibrium (the Gibbs phase rule). Premature K_4C_{60} formation implies that the $K_3C_{60}(111)$ islands are large compared to the diffusion length of surface K atoms on these grains at 180 °C. Hence, K atoms impinging on K_3C_{60} grains can nucleate K_4C_{60} (the heat of formation is 1.7 eV/K atom relative to K metal and solid C_{60}). At the surface there is less steric hindrance to the lattice expansion necessary for the transformation to bct K_4C_{60} , so the activation energy for K_4C_{60} nucleation is reduced. The fact that the K_4C_{60} phase could not be converted into K_3C_{60} by annealing, even at 400 °C, is consistent with the nearly identical heats of formation of the two phases.⁷ Annealing to higher temperatures (550 °C) in an attempt to obtain phase-pure K_3C_{60} resulted in film desorption. Thus growth in an open system cannot reach the same final state as that achieved under bulk crystal growth in a closed system. Nonequilibrium growth is a fundamental problem for vapor-phase fulleride formation;¹⁴ it is unlikely that a single-phase sample can be

grown even when the global stoichiometry corresponds to one of the line compounds. Evidence of the multiphase character of thin-film samples can be seen in the broad HOMO-derived features of all K_xC₆₀ spectra for $x \approx 3$.^{1-5,8} Multiphase growth would be exacerbated on C₆₀ surfaces rich in nucleation sites such as steps, grain boundaries, and other defects that are common to films grown at 300 K.¹²

Despite phase coexistence, it is straightforward to obtain the line shape of K₃C₆₀ by subtracting the α -phase contributions from spectra obtained for K_xC₆₀ with $x \leq 2.5$, i.e., before the K₄C₆₀ phase appeared. To do so, we represent the α phase by the $x = 0.1$ spectrum of Fig. 1, even though it includes a small amount of K₃C₆₀ emission. The only adjustable parameter in these line-shape subtractions is the amount of the two phases, and these must be consistent with x values determined from core-level and LUMO intensities (i.e., the line shapes and peak positions are not allowed to vary). Since the spectra include contributions from only two phases (α -C₆₀ and K₃C₆₀), the x values uniquely determine the relative contributions of each phase. For example, a sample with $x = 1.3$ must be constructed from 42.5% K₃C₆₀ and 57.5% K_{0.1}C₆₀. Such analysis does not uniquely determine the contributions when three phases are present in the film. Even for three-phase films, however, the x values limit the allowed range of contributions from each phase. For x approaching 4, the analysis is again straightforward because the amount of α phase is negligible.

The top panel of Fig. 2(a) shows the measured spectrum from $x = 2.2$, a scaled α -C₆₀(111) curve, and the K₃C₆₀(111) curve (bold) produced by subtraction. Subtractions carried out using results from samples for x values between 0.9 and 2.5 and for $h\nu = 16.8$ and 21.2 eV gave consistent peak positions, widths, and line shapes for the K₃C₆₀(111) spectrum. Figure 2(b) shows the spectrum for $x = 3.7$, where the K₄C₆₀ spectrum (bold) was that of Fig. 1 for $x = 4.2$, and the K₃C₆₀ emission was equivalent to that of Fig. 2(a); a 10% α -C₆₀ contribution was also subtracted.

Figure 2 (or the raw data for $x < 2.5$ for that matter) shows that K₃C₆₀(111) is characterized by a distinct Fermi edge and LUMO-derived features at 0.3 and 0.7 eV. While the LUMO feature has previously been described as a parabolic band characteristic of a free-electron metal,³ the present results show that this is not the case. Except for the LUMO-derived band, the bandwidths in K₃C₆₀ are only slightly different from those for C₆₀, and the ratio of the integrated LUMO to HOMO intensities is half of that for K₆C₆₀. The number of states at E_F , $N(E_F)$, can be determined by assuming the integrated intensity of the half-filled LUMO band is 3 electrons/molecule. Hence, $N(E_F) = 3.6 \pm 0.2$ electrons/eV molecule (5.1×10^{-3} electrons/eV Å³).³ This is a lower limit on $N(E_F)$ because electron-energy-loss processes and experimental broadening of the resolution-limited feature at E_F will reduce the intensity at E_F . Indeed, the 0.3-eV feature could correspond to a Franck-Condon excitation of molecular vibrational modes. Losses on the order of

50% will bring the photoemission value of $N(E_F)$ into closer agreement with other measurements.¹⁵

Figure 2 shows calculated densities of states (DOS) for K₃C₆₀ and K₄C₆₀ that were determined using the local-density pseudopotential method.⁷ While such calculations correctly describe the global features of C₆₀, it is clear that they fail to describe the photoemission spectra

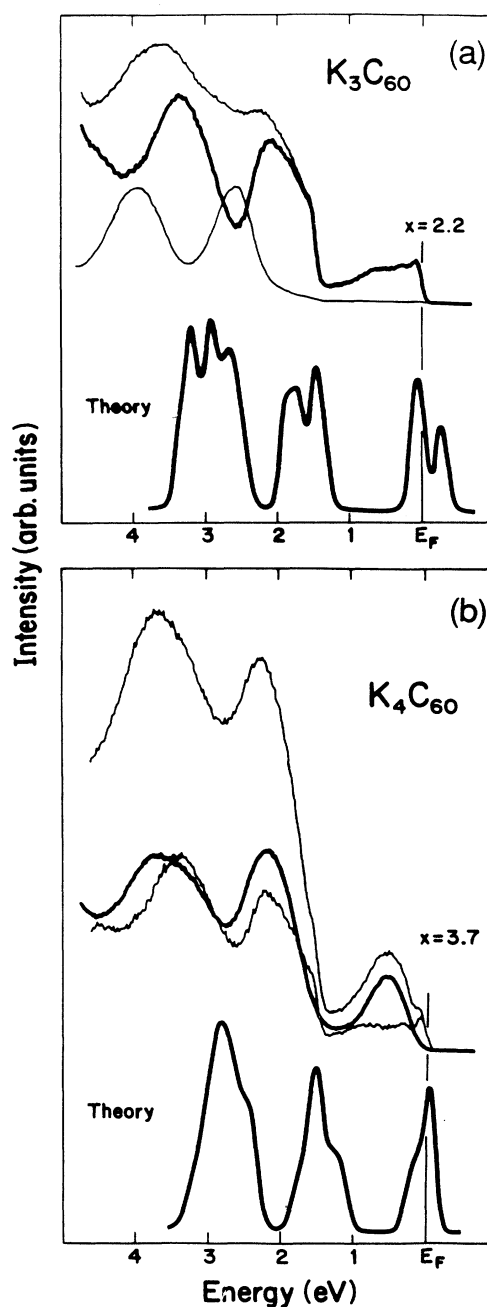


FIG. 2. (a) UPS spectrum for $x = 2.2$ derived from α -C₆₀(111) and K₃C₆₀(111) (bold) and the density of states for K₃C₆₀. (b) UPS spectrum for $x = 3.7$ derived from K₃C₆₀ and K₄C₆₀ (bold); a 10% contribution from α -C₆₀(111) is not shown. The bottom curve represents the density of states for K₄C₆₀.

near E_F for the fullerides. In particular, they predict a narrow peak in the LUMO-derived band of K_3C_{60} , while the experimental width of 1.2 eV is ~ 4 times larger. K_4C_{60} is predicted to be a metal but is seen to be an insulator. Experimentally, K_4C_{60} exhibits a peak centered 0.5 eV below E_F that accounts for four of the six states derived from LUMO. Away from E_F , the calculated widths of the HOMO and HOMO-1 features agree quite well with experiment for both fullerides.

Comparison of the two DOS's in Fig. 2 shows very similar peak positions and bandwidths for K_3C_{60} and K_4C_{60} , indicating the gross features of the DOS are insensitive to the precise values of the input parameters of the calculation. Indeed, there is no reasonable way within a one-electron picture to produce a large splitting of the threefold-degenerate LUMO that can be reconciled with photoemission. On the other hand, the results are consistent with a Mott-Hubbard-type insulator, where the lower Hubbard band is split by $U \sim 1.5$ eV from the upper band. A value of 1.5 eV for an effective molecular parameter U for K_4C_{60} is reasonable given that similar values have been invoked for C_{60} and K_6C_{60} to explain the gap determined from optical absorption and photoemission,⁸ the Auger spectrum,⁶ and the fact that all of the Na fullerides are insulators.¹⁶ Transport measurements also show that K_4C_{60} is an insulator, not a metal as predicted by theory.^{7,14}

For $K_3C_{60}(111)$, the LUMO-derived intensity can be interpreted as reflecting emission from a narrow quasiparticle band at E_F plus a broad spectral distribution centered at 0.7 eV that is associated with the incoherent part of the electronic spectral function. This broad spectral feature is near where the lower Hubbard band of K_4C_{60} is observed. While there is a distinct gap for K_4C_{60} , there is no evidence for a pseudogap between upper and lower Hubbard bands for K_3C_{60} .

The fulleride phases of K straddle a metal-insulator transition, and the results are similar to those reported by Fujimori *et al.*¹⁷ for a family of transition-metal oxides near a metal-insulator transition. They found a transfer of spectral weight from a quasiparticle peak at E_F to a Hubbard-like band below E_F as the strength of the electron-electron interaction U was increased. Here we see different distributions of spectral weight corresponding to different K content of the fulleride. The transfer of spectral weight from a quasiparticle to an incoherent peak is a mechanism proposed recently¹⁸ for the metal-insulator transition in a strongly correlated electronic system as an alternative to the opening of a pseudogap.

We do note that a broadening of the K_3C_{60} LUMO structure could be induced by plasmon losses and intra-LUMO transition losses ($\hbar\omega \cong 0.2-0.5$ eV) as well as multiple molecular vibrational losses ($\hbar\omega_{\text{vib}} = 0.04-0.2$ eV). However, no loss structures corresponding to the 0.7-eV feature of LUMO have been observed for the valence-band or core-level features.

Finally, it has been suggested that surface effects could produce a nonmetallic top layer on a K_3C_{60} film.¹⁹ This insulating layer would contribute emission at ~ 0.5 eV. We have investigated surface effects by varying the probe

depth of photoemission, finding no evidence that the surface layer of molecules differs from underlying layers in terms of its valence-band distribution. Thus each fullerene, whether at the surface or in the bulk, is sufficiently coordinated with K to have the same number of electrons in the LUMO band. A layer with different LUMO occupation does not exist. Figure 3 shows a comparison of LUMO features for $h\nu = 21.2$ and 16.8 eV. This change in photon energy produces a $\sim 60\%$ increase in the mean free path λ , assuming $\lambda \sim E^{-2}$. The results are essentially identical. Moreover, the top pair demonstrates that the K_4C_{60} phase is not confined to the surface but grows into the film. In addition, we have conducted studies of K_3C_{60} using polar-angle-dependent x-ray photoemission. In this case, 95% of the signal came from within ~ 2.5 molecular layers at grazing emission and nine molecular layers at normal emission. These results, as well as comparisons of K concentrations determined from LUMO ($\lambda \cong 8$ Å) and K $2p$ ($\lambda \cong 24$ Å) intensities, showed no evidence for surface effects. The agreement between the results shown in Fig. 1 and the $h\nu = 110$ -eV spectra of Ref. 3 indicate the insensitivity of these spectra to probe depth changes. We see no evidence of enhanced insulating character for the more surface-sensitive ($h\nu = 21.2$ eV) results, as has been reported elsewhere.¹⁹ It may be that the changes observed were a result of

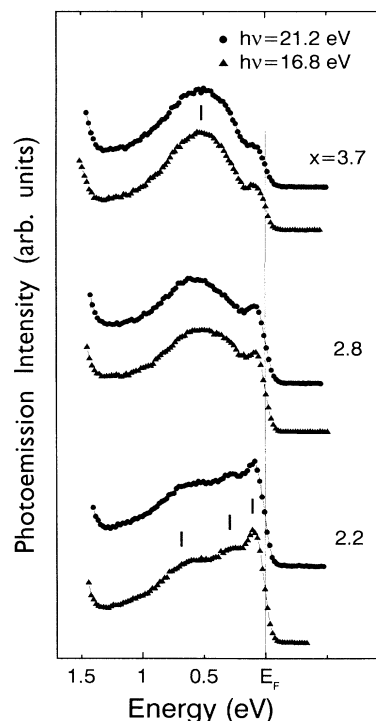


FIG. 3. LUMO-derived emission demonstrating that the surface layer of K_xC_{60} has the same character as the lower layers (λ increases $\sim 60\%$ between 21.2 and 16.8 eV). The 0.3- and 0.7-eV features ($x = 2.2$) are intrinsic to K_3C_{60} ; the 0.5-eV feature ($x = 3.7$) reflects the K_4C_{60} phase.

differences in film growth conditions, a greater abundance of K₄C₆₀, and uncertainties in x .

By isolating the electronic signatures of K₃C₆₀ and K₄C₆₀, these results have raised fundamental questions pertinent to electron correlation and superconductivity. Of the fullerides, only the binary or ternary fullerides with the A₃C₆₀ structure have been shown to be metallic;²⁰ all others show Hubbard-like band splitting.¹⁶ None of the higher fullerenes have been shown to be metallic when doped with K.²¹ It remains to be determined how the interplay of a half-filled band with 3 electrons/molecule and the fulleride structure gives rise

to the metallic character of the "anomalous" A₃C₆₀ fullerides. Clearly, these results show the importance of electron-electron correlation for the K_{*n*}C₆₀ phases and that the ground-state electronic properties are very different for different phases.

This work was supported by the National Science Foundation, the Office of Naval Research, and the Robert A. Welch Foundation. Interactions with A. Fujimori are gratefully acknowledged, as is correspondence with A. A. Lucas and M. Gelfand.

¹P. J. Benning *et al.*, *Science* **252**, 1417 (1991).

²G. K. Wertheim *et al.*, *Science* **252**, 1419 (1991).

³C. T. Chen *et al.*, *Nature* **352**, 603 (1991).

⁴J. Fink *et al.*, in *Fullerenes: Status and Perspectives*, edited by C. Taliano, G. Ruani, and R. Zamboni (World Scientific, Singapore, 1992), p. 161.

⁵T. Takahashi *et al.*, *Phys. Rev. Lett.* **68**, 1232 (1992).

⁶R. W. Lof *et al.*, *Phys. Rev. Lett.* **68**, 3924 (1992).

⁷J. L. Martins and N. Troullier, *Phys. Rev. B* **46**, 1766 (1992); see also S. Saito and A. Oshiyama, *ibid.* **44**, 11 537 (1991); Y.-N. Xu, M. Z. Huang, and W. Y. Ching, *ibid.* **44**, 13 171 (1991); M. P. Gelfand and J. P. Lu, *Phys. Rev. Lett.* **68**, 1050 (1992); S. Satpathy *et al.*, *Phys. Rev. B* **46**, 1773 (1992); S. C. Irwin and W. E. Pickett, *Science* **254**, 842 (1992).

⁸P. J. Benning *et al.*, *Phys. Rev. B* **45**, 6889 (1992).

⁹J. H. Weaver *et al.*, *Phys. Rev. Lett.* **66**, 1741 (1991).

¹⁰P. A. Heiney *et al.*, *Phys. Rev. Lett.* **66**, 2911 (1991).

¹¹R. M. Fleming *et al.*, *Nature* **352**, 701 (1991).

¹²Y. Z. Li *et al.*, *Science* **253**, 429 (1991).

¹³F. Stepniak, P. J. Benning, D. M. Poirier, and J. H. Weaver, *Phys. Rev. B* (to be published).

¹⁴J. H. Weaver *et al.*, *J. Phys. Chem. Solids* **53**, 1707 (1992).

¹⁵R. Tycko *et al.*, *Science* **253**, 884 (1991).

¹⁶C. Gu *et al.*, *Phys. Rev. B* **44**, 6348 (1992).

¹⁷A. Fujimori *et al.*, *Phys. Rev. Lett.* **69**, 1796 (1992).

¹⁸A. Khurana, *Phys. Rev. B* **40**, 4316 (1989).

¹⁹G. K. Wertheim *et al.*, *Solid State Commun.* **83**, 785 (1992).

²⁰R. C. Haddon, *Acc. Chem. Res.* **25**, 127 (1992).

²¹S. Hino, *Chem. Phys. Lett.* **190**, 169 (1992).